PHYSICAL REVIEW B **78**, 075434 (2008)

# Diodelike effect in nanoelectromechanical shuttle devices

Rui-Qiang Wang,[1,2] Baigeng Wang,[1] and D. Y. Xing[1]

[1]*National Laboratory of Solid State Microstructures and Department of Physics, Nanjing University, Nanjing 210093, China*

[2]*Institute for Condensed Matter Physics, School of Physics and Telecommunication Engineering, South China Normal University, Guangzhou, 510006, China*

(Received 18 March 2008; revised manuscript received 13 June 2008; published 22 August 2008)

We have analyzed the effect of bias-voltage polarities on the shuttle instability in an asymmetrically nanoelectromechanical single-electron transistor (NEM-SET) using the Wigner phase space approach. The electric-field-induced shift in oscillation equilibrium position together with the asymmetrical tunneling rate leads to the symmetry breaking of electron occupations in the quantum dot for positively and negatively biased directions. The symmetry-broken occupations make the works done by the electric field in different biased directions unequal. As a consequence, the threshold voltage for the onset of shuttle instability is lower for a positive bias voltage than for a negative one. Between two thresholds, the NEM-SET device exhibits a pronounced rectification effect.

DOI: 10.1103/PhysRevB.78.075434 PACS number(s): 85.85.+j, 73.23.Hk, 85.35.Be

## I. INTRODUCTION

Recently, a nanoelectromechanical single-electron transistor (NEM-SET), consisting of a movable nanometer quantum dot (NQD) or an island coupled to the emitter and collector leads, has attracted growing attention. Distinguished from conventional SET, it combines single-electron transport with mechanically oscillating degree of freedom and so it may give rise to a revolution in applications. Many studies proposed the NEM-SET as a detector of very small force,[1] small magnetic field,[2,3] and spin state[4] and also as data storage[1] and nanomechanical computer.[5]

Since the tunneling amplitude in NEM-SET devices is exponentially dependent upon the spatial displacement of NQD, the current flow through the setup is greatly sensitive to the NQD motion.[4,6] If the applied bias is small, the central NQD will oscillate almost in the vicinity of the zero point. Thus the electron tunnels into the dot from the emitter and off to the collector without much involvement of the excitation of island vibration.[7,8] This is the so-called tunneling transport, where the electronic current shows the usual features of mechanically assisted tunneling transport. On the contrary, if the applied bias is large enough, the charged island will be accelerated by electric force and obtain energy from the electronic current every time an electron transfers from one lead to the other.[9] As a consequence the oscillation amplitude of the island becomes larger and larger and finally develops into a shuttle instability, where electrons are transported from one electrode to the other with a probability of essentially 1 to be offloaded at the first approach to the drain electrode. This is a novel shuttle transport, a significant feature of which is that the current value depends only on the frequency of the oscillator. In fact, this bias-induced tunneling-shuttling transition is a process where bias voltage makes the motion of island excited from vibrational ground state. The shutting mechanism gives rise to a sharp step in *I*-*V* relation at a certain threshold voltage,[10,11] which signals the transition from the tunneling transport to the shuttling transport.

So far there have been many investigations on the shuttle phenomena. Although in experimental aspect Park *et al.*[7] provided a possible shuttle device with single-molecule $C_{60}$, the realization of a nanomechanical shuttle still depends on a time-dependent ac driving voltage.[12–14] In an exciting report, Kim *et al.*[5,15] recently suggested that the self-excited mechanical oscillation can be generated without any ac driving field. In theoretical aspect, the investigation of shuttle instability has also become a topic. Novotný *et al.*[16] extended an early classical description[9,10] to a full numerical quantum treatment. In order to study the quantum shuttle phenomena analytically, quasiclassical theory, incorporating the generalized master equation and Wigner phase space technology, was extensively adopted.[2,3,17–20] Many studies[3,16–18] reported the influences of bias voltage and damping rate on the shuttle threshold, above which a dynamic instability occurs and the center-of-mass motion of the dot develops into a stable limit cycle. Furthermore, Fedorets *et al.*[2] pointed out that the shuttle instability is also sensitive to applied magnetic field. Motivated by these reports in literature, we recently studied a magnetic shuttle device[20] and showed that the bias-voltage threshold is relevant to the relative directions of magnetization in two ferromagnetic leads.

Shuttle device as a candidate of future function element was proposed as a rectifier in studies.[21,22] Pistolesi and Fazio[21] remarked that the charge shuttle driven by a time-dependent bias voltage can behave as an interesting rectifier even for very low frequency because of the nonlinear dynamics of nanomechanical devices. In the present paper, we consider the shuttle instability of the tunneling-shuttling transition through an NEM-SET structure. We exhibit that the joint effect of the asymmetric setup and the shift in oscillation equilibrium position by the electric field will give rise to the symmetry-broken occupation in the NQD between the positive bias voltage (PBV) and the negative bias voltage (NBV). If the vibrational equilibrium position of the island shifts to the side with a small tunneling rate in one biased direction, the oscillator is easier to transit from a tunneling regime to a new shuttling regime than in the opposite biased direction. Thereafter, the onsets of the dynamic instability (or the threshold voltages) are different for two biased directions at the same damping. In between two thresholds, this device is shown to have an ideal diodelike rectification effect. If either the asymmetry or the shift disappears, the rectification will vanish. In Sec. II we address a theoretical model within the framework of quantum master equation together with Wigner phase space. In Sec. III we discuss an interesting diodelike rectification effect by analyzing the effective potential and probability distribution of oscillator in Wigner representation. The electron occupation in the island is analyzed in Sec. IV. Finally, a short summary is given in Sec. V.

## II. THEORETICAL MODEL AND METHOD

We consider a typical Hamiltonian for the NEM-SET,

$$H=\sum_{k,\alpha}(\varepsilon_{k,\alpha}-\mu_\alpha)c^\dagger_{k,\alpha}c_{k,\alpha}+\varepsilon_0 d^\dagger d+\sum_{k,\alpha}[T_\alpha(X')c^\dagger_{k,\alpha}d+\text{H.c.}]+P'^2/2M+M\omega_0^2X'^2/2-e\epsilon X'd^\dagger d+H_{\text{damp}}. \quad (1)$$

The first three terms are similar to the conventional SET Hamiltonian, i.e., two noninteracting electron reservoirs $\alpha\in L,R$ as an emitter and a collector, the single energy level $\varepsilon_0$ of the NQD, and the couplings between the NQD and the reservoirs. $c^\dagger_{k,\alpha}(c_{k,\alpha})$ creates (annihilates) an electron in lead $\alpha$ with energy $\varepsilon_{k,\alpha}$ and wave vector $k$; $d^\dagger$ is the creation operator of electrons in the dot. Unlike the conventional SET, where the quantum dot (or island) is static, the NQD in the NEM-SET is suspended between the emitter and the collector. Its center-of-mass motion is assumed to be confined in a harmonic potential with mass $M$ and vibration frequency $\omega_0$. So the tunneling amplitude, $T_{L(R)}(X')=T_{L(R)}\exp(\mp X'/\lambda')$, with $\lambda'$ as the electron tunneling length, is exponentially dependent upon the displacement operator $X'$. The electrochemical potential $\mu_{L,R}=\pm eV/2$ is measured with respect to unbiased Fermi surface, where $V$ is the bias voltage and $e>0$ is the electron charge. We define the positive bias voltage as the case that the left lead serves as the emitter and the right lead as the collector ($eV>0$). We define the negative bias voltage as the opposite process ($eV<0$). When the dot is charged, the electrostatic potential $e\epsilon X'$ arises where the electric-field strength $\epsilon$ between the emitter and the collector is simulated as parallel-plate capacitor $\epsilon=V/L$, with $L$ as the distance between reservoirs.[9,10] As a result, the equilibrium position of the harmonic oscillator is shifted along the electric-field direction. The last term, $H_{\text{damp}}=\Sigma_p\varepsilon_p b^\dagger_p b_p+g_pX'(b_p+b^\dagger_p)$, represents the damping environment modeled by bosonic heat bath and its coupling to the oscillator motion.[23]

For convenience, we measure all lengths in units of the zero-point oscillation amplitude $x_0=\sqrt{\hbar/M\omega_0}$ and all energies in units of $\hbar\omega_0$. The operators $x=X'/x_0$, $p=x_0P'/\hbar$, and $\eta=e\epsilon x_0/\hbar\omega_0$ are dimensionless displacement, momentum, and electric field, respectively. The Liouville–von Neumann equation is used to derive the quantum master equation for the full Hamiltonian [Eq. (1)] in terms of the full density matrix $\varrho(t)=\rho_L\otimes\rho_R\otimes\rho_{\text{therm}}\otimes\rho_{\text{joi}}$, where $\rho_{\text{joi}}$ is the electron-oscillator joint density-matrix operator. Using the standard Born and Markov approximations,[2,16,17,24] we trace out the degrees of freedom of the thermal bath and the electron in leads and finally find a generalized Markovian master equation for the joint density matrix $\rho_{\text{joi}}$,

$$\frac{\partial\rho_{\text{joi}}}{\partial t}=-i\left[\frac{1}{2}(p^2+x^2)+(\varepsilon_0-\eta x)d^\dagger d,\rho_{\text{joi}}\right]+\int d\varepsilon\{\Gamma_L D[d^\dagger e^{-x/\lambda}]\rho_{\text{joi}}f^+_L(\varepsilon)\}+\Gamma_L D[de^{-x/\lambda}]\rho_{\text{joi}}f^-_L(\varepsilon)+\Gamma_R D[d^\dagger e^{x/\lambda}]\rho_{\text{joi}}f^+_R(\varepsilon)+\Gamma_R D[de^{x/\lambda}]\rho_{\text{joi}}f^-_R(\varepsilon)-\frac{i\gamma}{2}[x,\{p,\rho_{\text{joi}}\}]-\frac{\gamma}{2}[x,[x,\rho_{\text{joi}}]], \quad (2)$$

where the notation $D$ is defined as $D[\xi]\rho_{\text{joi}}=\xi\rho_{\text{joi}}\xi^\dagger-\frac{1}{2}(\xi^\dagger\xi\rho_{\text{joi}}+\rho_{\text{joi}}\xi^\dagger\xi)$, with $\xi$ as an arbitrary operator, and $[\cdot,\cdot]$ and $\{\cdot,\cdot\}$ stand for the commutator and anticommutator, respectively. $\Gamma_\alpha(\varepsilon)=2\pi\Omega_\alpha(\varepsilon)|T_\alpha|^2$ is the tunneling rate between the NQD and the emitter (or collector), with $\Omega_\alpha(\varepsilon)$ as the density of states in lead $\alpha$. In the wide-band approximation, the tunneling rate is independent of energy. $f^+_\alpha(\varepsilon)=\text{Tr}[c^\dagger_{k,\alpha}c_{k,\alpha}\rho_\alpha]=[1+\exp(\frac{\varepsilon-\mu_\alpha}{k_BT})]^{-1}$ is a Fermi function and $f^-_\alpha(\varepsilon)=1-f^+_\alpha(\varepsilon)$. The dimensionless dissipation rate $\gamma\ll 1$ describes the weak damping process of the oscillator motion. We are interested in the transition from tunneling to shuttling regime, in which a large bias voltage $|eV|\gg\hbar\omega_0,\varepsilon_0,k_BT$ is required and so the Fermi function reduces to the unit step function. In steady state, it is sufficient to consider only the diagonal elements of joint density matrices in electron subspace:[16] $\rho^0_{\text{osc}}=\langle 0|\rho_{\text{joi}}|0\rangle$ and $\rho^1_{\text{osc}}=\langle 1|\rho_{\text{joi}}|1\rangle$.

A useful tool for analyzing the quantum dynamic system in phase space is the Wigner distribution function, defined as[25] (take $\hbar=1$)

$$W_{0(1)}(x,p)=\frac{1}{2\pi}\int_{-\infty}^{\infty}dy\left\langle x-\frac{y}{2}\left|\rho^{0(1)}_{\text{osc}}\right|x+\frac{y}{2}\right\rangle e^{ipy}. \quad (3)$$

If the leads are biased by the PBV, the density matrices $\rho^0_{\text{osc}}$ and $\rho^1_{\text{osc}}$ can be mapped into the following charge-resolved Wigner representation respectively:

$$\frac{\partial W_0}{\partial t}=\left[\left(x+\frac{\eta}{2}\right)\partial_p-p\partial_x+L_\gamma\right]W_0+\Gamma_R e^{(2x+\eta)/\lambda}W_1-\Gamma_L e^{-(2x+\eta)/\lambda}\sum_{n=0}^{\infty}\frac{(-1)^n}{(2n)!}\left(\frac{1}{\lambda}\right)2n\frac{\partial^{2n}W_0}{\partial_p^{2n}}, \quad (4)$$

$$\frac{\partial W_1}{\partial t}=\left[\left(x-\frac{\eta}{2}\right)\partial_p-p\partial_x+L_\gamma\right]W_1+\Gamma_L e^{-(2x+\eta)/\lambda}W_0-\Gamma_R e^{(2x+\eta)/\lambda}\sum_{n=0}^{\infty}\frac{(-1)^n}{(2n)!}\left(\frac{1}{\lambda}\right)2n\frac{\partial^{2n}W_1}{\partial_p^{2n}}, \quad (5)$$

where $L_\gamma=\gamma\partial_p p+\frac{\gamma}{2}\frac{\partial^2}{\partial_p^2}$ and the origin of $x$ axis is shifted to the point $x=\frac{\eta}{2}$. In order to find the stationary solution $\frac{\partial W_{0(1)}}{\partial t}=0$, it is convenient to switch them to the polar coordinate, $X=x/\lambda=A\sin\theta$ and $P=p/\lambda=A\cos\theta$, with $\lambda=\lambda'/x_0$. Note that $x,p$ are numbers rather than operators from now on. The quantum commutation relation $[x,p]$ is reflected in $2n$-order differential terms. $n=0$ implies that the commutation relation of $[x,p]$ vanishes, which corresponds to the classic picture. In what follows, we make perturbation expansion in the small parameters $\eta/\lambda, 1/\lambda^2, \gamma \ll 1$ to the second order ($n = 0,1$), so the dynamic system is analyzed in the quasiclassical picture.[2,16,17]

The expectation value of the electron current is determined by the total (discharged $W_0$ and charged $W_1$) states of the vibrational degree of freedom, $W_+ = W_0 + W_1$, whereas $W_- = W_0 - W_1$ is related to the shuttling correlations between the charge state and the mechanical state of the island. Using the projector $P_\theta f(\theta) \equiv \frac{1}{2\pi}\int_0^{2\pi} f(\theta) d\theta$ and complementary projector $\vartheta \equiv 1 - P_\theta$, it is easy to find a closed equation $\partial_\theta W_+ = \pounds W_+$. Here

$$\pounds = \gamma \partial_P P + \frac{\gamma}{2\lambda^2}\frac{\partial^2}{\partial_P^2} + \frac{1}{4\lambda^4}[\Gamma_L(X) + \Gamma_R(X)]\frac{\partial^2}{\partial_P^2} + \left\{\frac{d}{2\lambda}\partial_P + [\Gamma_L(X) - \Gamma_R(X)]\frac{1}{4\lambda^4}\frac{\partial^2}{\partial_P^2}\right\} G_-, \quad (6)$$

with $\Gamma_{L(R)}(X) = \Gamma_{L(R)} e^{\mp(2X + \eta/\lambda)}$ and $W_- = G_- W_+$. $G_-(A,\theta)$ is a $2\pi$ periodic function of the variable $\theta$ and it satisfies the equation

$$\partial_\theta G_- = -[\Gamma_R(X) + \Gamma_L(X)]G_- + [\Gamma_R(X) - \Gamma_L(X)]. \quad (7)$$

$G_-(A,\theta)$ is related to the electron occupation in the dot through $n(A,\theta) = 1/2[1 - G_-(A,\theta)]$,[17] which is the net charge in the dot due to the incoming charge from the left minus the outgoing charge to the right. In the leading-order approximation, the equation for $W_+$ can be reduced to the Fokker-Planck equation.[2,3,17] Its solution reads

$$W_+ \approx \bar{W}_+(A) = Z^{-1} \exp\left[-\int_0^A \frac{f(A')}{D(A')} dA'\right], \quad (8)$$

with a normalization constant $Z$ determined by an equality $2\pi\int_0^\infty \bar{W}_+(A) A dA = 1$. Here the amplitude-dependent diffusive component is

$$D(A) = \frac{\gamma}{4\lambda^2} + \frac{1}{4\lambda^4} P_\theta \cos^2\theta \Bigg\{\Gamma_L(X) + \Gamma_R(X) + [\Gamma_L(X) - \Gamma_R(X)]G_- + \left(\frac{\eta}{2\lambda}\right)^2 P_\theta \cos\,\theta\{G_- \partial_\theta^{-1} \vartheta \cos\,\theta G_-\}\Bigg\}. \quad (9)$$

The amplitude-dependent driving component is $f(A) = f_{\mathrm{damp}}(A) - f_{\mathrm{el}}(A)$. with the damping force and electric-field force written respectively as

$$f_{\mathrm{damp}}(A) = A\frac{\gamma}{2}, \quad f_{\mathrm{el}}(A) = -\frac{\eta}{2\lambda} P_\theta \cos\,\theta G_-. \quad (10)$$

From the continuity equation for the charge, the stationary current through the system is given by

$$I = e\,\mathrm{Tr}[\Gamma_{L\sigma} e^{-2x/\lambda}\rho_0] = \frac{e}{2}\Gamma_L \int_0^\infty W_+ A dA \int_0^{2\pi} d\theta e^{-(2A\sin\,\theta + \eta/\lambda)} \times (1 + G_-). \quad (11)$$

When the dynamical system is biased negatively, one must return to Eq. (2) and rederive the formula. We find that the above formulas are also suitable for the NBV case only when exchanging $\Gamma_L(X) \Leftrightarrow \Gamma_R(X)$ and setting $X = A\,\sin(\theta + \pi)$.

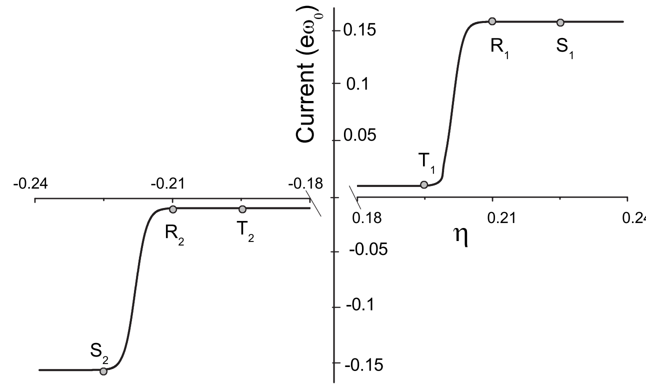


FIG. 1. $I$-$\eta$ curves. The parameters are $\gamma = 0.01$, $\chi = 0.8$, $\Gamma = 0.1$, and $\lambda = 5$.

### III. ANALYSIS OF THE RECTIFICATION EFFECT

We consider a shuttle structure with an asymmetry factor defined as $\chi = (\Gamma_L - \Gamma_R)/\Gamma$ and $\Gamma = \Gamma_L + \Gamma_R$. Based on the above theory, we depict the $I$-$\eta$ curves in Fig. 1. It is found that when $\eta$ increases negatively or positively, both the curves exhibit an abruptly increasing current at a certain threshold voltage. The threshold value is the transition point from the tunneling regime to the shuttling regime. When $|\eta|$ is smaller than both thresholds (e.g., at points $T_1$ and $T_2$), the currents of both the PBV and the NBV are very small, proportional to $\Gamma_L\Gamma_R/(\Gamma_L + \Gamma_R)$. When $|\eta|$ is greater than both thresholds (e.g., at points $S_1$ and $S_2$), the currents are very large and given by $I = ef$, with $f \equiv \omega_0/2\pi$ as the self-oscillation frequency of the NQD. It is interesting to find that the threshold of electric field $|\eta|$ is lower for the PBV than for the NBV. Thus there appears a new region (e.g., at points $R_1$ and $R_2$) between the two thresholds. In this region the shuttling transport with large current dominates the electronic transport for the PBV case, while the tunneling transport with very smaller current does for the NBV case. This means that electron current will flow through the NEM-SET devices in one biased direction but will almost be prohibited in the other biased direction at this new region. In other words, the present NEM-SET exhibits an ideal diodelike rectification effect. We term this new region between two thresholds as rectification region. In the following we evaluate the realistic current by taking the parameters from the experiment.[7] The narrowest gap between the two leads is $L = 1$ nm, the harmonic force constant is $K = 70$ N m$^{-1}$, and the vibrational frequency of the molecule $C_{60}$ is $f = 1.2$ THz. Thus, one can obtain $\hbar\omega_0 \approx 5$ meV and $x_0 \approx 10^{-3}$nm. After recovering the unit, the threshold voltage is about 1 V ($\eta = 0.2$) for the PBV and $-1.1$ V ($\eta = -0.22$) for the NBV, and the shuttling current is about 190 nA and the tunneling current is about 9 nA. In order to detect the rectification in experiment, the single-molecule setup[7,26] is the most possible candidate.

The above transport features are closely related to the oscillator behavior. In what follows we will analyze the

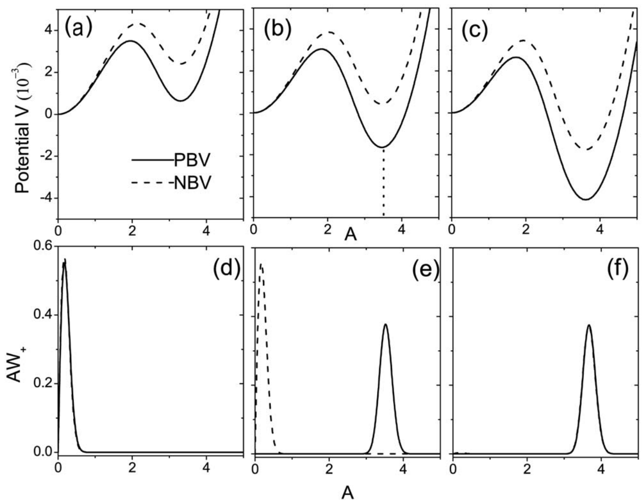


FIG. 2. Effective potentials $V(A)$ and corresponding amplitude probability distributions $AW_+$ for the PBV (solid line) and NBV (dashed line) cases. The solid lines in (a) and (d), (b) and (e), and (c) and (f), respectively, correspond to points $T_1$, $R_1$, and $S_1$ in Fig. 1, and the dashed lines correspond to points $T_2$, $R_2$, and $S_2$. The other parameters are the same as in Fig. 1.

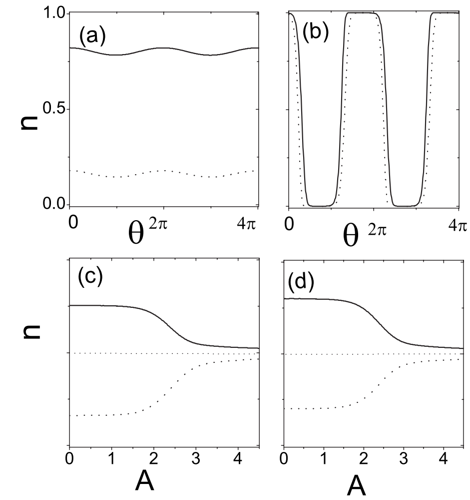


FIG. 3. The net electron occupation $n(\theta)$ in the NQD as a function of oscillating phase $\theta$ for (a) $A=0.5$ and (b) $A=3.5$ ; $n(A)$ as a function of $A$ (c) with and (d) without the shift in equilibrium position. The other parameters are $\eta=0.2$, $\chi=0.6$, $\Gamma=0.1$, and $\lambda=5$. The solid lines correspond to the PBV and the dashed lines to the NBV.

probability distribution of the oscillator in the Wigner phase space. In the quasiclassical regime ($\lambda \gg x_0$), the competition between work functions $W_{\rm el}(A)=\int_0^A f_{\rm el}(A')dA'$ and $W_{\rm damp}(A)=\int_0^A f_{\rm damp}(A')dA'$, done by $f_{\rm damp}$ and $f_{\rm el}$ respectively, directly determines whether the oscillator is in the tunneling or the shuttling regime. It is convenient to define an effective potential[18] $V(A)=W_{\rm damp}(A)-W_{\rm el}(A)$ as a function of $A$. In Fig. 2, we plot the effective potential $V(A)$ in the upper panels and the corresponding probability distribution function $AW_+(A)$ in the lower panels as functions of oscillation amplitude $A$. In Figs. 2(a) and 2(d), 2(b) and 2(e), 2(c) and 2(f) the electric fields respectively correspond to the points $T_1$, $R_1$, and $S_1$ for the solid curves and points $T_2$, $R_2$, and $S_2$ for the dashed lines in Fig. 1. In the Figs. 2(a)–2(c), the global potentials present a double-well structure, one well located around the origin and the other at $A_{\rm cl}$, which is classic limit cycle shown by the vertical dotted line. The limit cycle is mainly determined by dynamic equilibrium condition $f(A_{\rm cl})=0$ and $f'(A_{\rm cl})>0$. With $|\eta|$ increasing in Figs. 2(a)–2(c), the potential heights between the double well change relatively, resulting in the altering of distribution function peaks. When $|\eta|$ is smaller, the NQD oscillates in the ground state with a small amplitude, indicated by the $AW_+(A)$ peaks in Fig. 2(d) located around the origin. This is because the energy pumped from electronic current into the oscillator is not enough to overcome damping environment, i.e., $W_{\rm el}<W_{\rm damp}$. When $|\eta|$ goes up and arrives at Fig. 2(b), there is an essential change for the PBV case because of $W_{\rm el}>W_{\rm damp}$ [or $V(A_{\rm cl})<0$]. In a cycle of the island oscillating, the excess energy is available for the oscillator to enlarge its amplitude for the PBV case. As shown in Fig. 2(e) the distribution function peak has been shifted to the position $A_{\rm cl}$, which implies that the oscillator has entered into shuttling state. On the contrary, the distribution function in Fig. 2(e) for the NBV case (dashed line) remains at the origin owing to $V(A_{\rm cl})>0$, which shows that the oscillator is still in the tunneling regime. Therefore, for two biased directions the oscillator is located in different regimes. The shuttling transport with large shuttling current in the PBV dominates the electronic transport, while the tunneling transport with very small current does so in the NBV. When $|\eta|$ enhances further as shown in Fig. 2(c), the potentials for both the PBV and the NBV are negative, so both the probability distributions of the oscillator are located at around $A_{\rm cl}$ [see Fig. 2(f)]. In this potential both transports are shuttle type. It is noticed that in Figs. 2(a)–2(c) the solid lines are always lower than the dashed lines owing to $W_{\rm el}^P(A)>W_{\rm el}^N(A)$, where the superscripts denote the PBV and NBV. Difference in potential for two biased directions is very important in the arising of the rectification effect. In order to understand the underlying physics, we should analyze in detail the work $W_{\rm el}(A)$, which is closely related to the shuttling correlation $G_-$ or the occupation $n$ in the dot due to $f_{\rm el}(A)=-\frac{\eta}{2\lambda}P_\theta \cos\theta G_-$.

## IV. ANALYSIS OF THE ELECTRON OCCUPATION IN THE NQD

In what follows we will discuss the origin of $W_{\rm el}^P(A)>W_{\rm el}^N(A)$. It is needed to make a detailed comparison of the occupation in the shuttle dot between the PBV and the NBV cases. In Figs. 3(a) and 3(b) we exhibit the variation in net occupation $n(A,\theta)=1/2[1-G_-(A,\theta)]$ with oscillator phase $\theta$ for fixed amplitudes $A$. Because of $\Gamma_L(X)\gg\Gamma_R(X)$, $\Gamma_R(X)$ becomes the transport bottleneck. For the small $A$ as shown in Fig. 3(a), an electron easily tunnels into the dot from the left lead but cannot in time tunnel off to the right lead when the system is subject to the PBV. Therefore, the dot is in a majority-occupied state. On the contrary, in the NBV an electron easily tunnels out into the left lead but finds it hard to jump into the dot from the right lead, and so the dot presents a minority-occupied state. In this small amplitude, the electron transport is tunnel type. With increasing $A$, the tunneling rate exponentially increases and it is possible for the electron to directly shuttle from the emitter to the collector. Figure 3(b) shows obvious evidence for the system to enter the shuttling regime, independent of biased directions. The value averaged over $\theta$, $n(A)=1/4\pi\int_0^{2\pi}d\theta[1-G_{-}(A,\theta)]$, is illustrated in Figs. 3(c) and 3(d), in which it is close to 0.5 in the shuttling regime. This means that the dot carries an electron from the emitter to the collector and is empty on its return trip. For convenience, we assume the shuttle dot to be unshifted by the electric-field influence [i.e., setting $\Gamma_{L(R)}(X)=\Gamma_{L(R)}e^{\mp 2X/\lambda}$]. The corresponding curves for the PBV (solid line) and the NBV (dashed line) are indicated in Fig. 3(d). One can find that the curves are strictly symmetrical about $n=0.5$, or the shuttle correlation $G_{-}(A)\rightarrow -G_{-}(A)$, when $\eta\rightarrow -\eta$. From Eq. (10) we know the electric-field force acting on the oscillator $f_{\mathrm{el}}(A)$ is the same for both the PBV and the NBV since $\eta G_{-}$ remains unchanged when $\eta\rightarrow -\eta$. In this case, our calculations show that $W_{\mathrm{el}}^{P}(A)=W_{\mathrm{el}}^{N}(A)$ and the electronic current is $I(V)=-I(-V)$. However, in fact, in the realistic system under consideration, the equilibrium position of the NQD is shifted by the electric field [taking $\Gamma_{L(R)}(X)=\Gamma_{L(R)}e^{\mp(2X+\eta/\lambda)}$]. This shift makes $n(A)$ gradually get close to $n=0.5$ for the PBV and close to $n=0$ for the NBV. As a result, the curves exhibit asymmetry between the dashed line and the solid line in Fig. 3(c). This change can be understood by the following arguments: The electron transport is mainly determined by the tunneling between the right lead and the dot (bottleneck). If the system is based positively, the equilibrium position of oscillator shifts toward the right collector, which is favorable for unloading in time an electron out of the majority-occupied dot. In contrast, if the system is based negatively, the opposite shift is more unfavorable for loading an electron into the minority-occupied dot. Comparing Fig. 3(c) with Fig. 3(d), it is obvious that the symmetry is broken, i.e., $\eta G_{-}$ changes when $\eta\rightarrow -\eta$. In turn, the asymmetry breaking leads to the larger work done by electric field for the PBV compared with that for the NBV, i.e., $W_{\mathrm{el}}^{P}(A)>W_{\mathrm{el}}^{N}(A)$. As a result, the $I$-$V$ curve exhibits a rectification effect, $I(V)\neq -I(-V)$.

We plot the currents for three sets of parameters as a function of $|\eta|$ in Figs. 4(a)–4(c), where we put the PBV curves (solid lines) and the NBV curves (dashed lines) together for comparison. In the NBV case, the corresponding axes' labels are of opposite sign. Comparing Fig. 4(b) with Fig. 4(a), we find that with decreasing asymmetric factor $\chi$ the rectification regime becomes narrower because symmetry breaking becomes little and that the whole curves shift to the smaller electric field due to increase in $\Gamma_R$. Our calculations show that the rectification regime vanishes if the system structure is symmetrical (setting $\chi=0$). A comparison of Fig. 4(c) with Fig. 4(a) shows that smaller damping environment

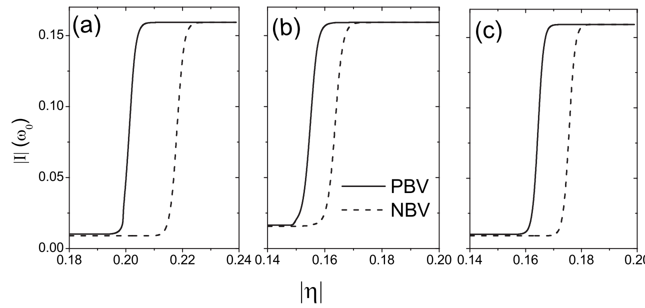


FIG. 4. $|I|$-$|\eta|$ curves in the PBV (solid lines) and NBV (dashed lines) cases with the parameters (a) $\chi=0.8$, $\gamma=0.01$; (b) $\chi=0.6$, $\gamma=0.01$; and (c) $\chi=0.8$, $\gamma=0.008$. The other parameters are the same as in Fig. 1.

makes both the curves shift to smaller $|\eta|$ together. When the dissipative rate $\gamma$ decreases, only a smaller electric field is required for the electronic transport to enter the shuttling regime. At the same time, $\gamma$ also changes the span of rectification regime by changing the threshold electric field.

## V. SUMMARY

We start from the quantum master equation to analyze electron transports through an asymmetric NEM-SET device by applying Wigner phase technique in the quasiclassical regime ($\lambda \gg x_0$). It is found that the shuttle instability in the asymmetric structure is closely dependent upon the biased direction (PBV or NBV). The onsets of the dynamical instability are different for positive and negative biases because of the symmetry-broken occupation in the dot, which makes the works done by the electric field in a shuttling cycle different for two biased directions. The work in the PBV is larger than that in the NBV at the same dissipative environment, so the threshold for the PBV is smaller compared with the one for the NBV. Between two thresholds, there appears an interesting diodelike rectification effect because the positive onset voltage is lower than the negative one. If either the asymmetry or the shift disappears, the rectification will vanish. In the deep quantum regime ($\lambda \sim x_0$), it is needed to take into account the higher-order terms or adopt full numerical calculation as done in Ref. 16. However, we expect that the rectification can remain in the deep quantum regime, although it may be somewhat destroyed by stronger quantum effect.

## ACKNOWLEDGMENTS

This work was supported by the National Natural Science Foundation of China under Grant No. 90403011 and also by the State Key Program for Basic Researches of China under Grants No. 2006CB921803 and No. 2004CB619004.

[1] H. G. Craighead, Science **290**, 1532 (2000).
[2] D. Fedorets, L. Y. Gorelik, R. I. Shekhter, and M. Jonson, Phys. Rev. Lett. **95**, 057203 (2005).
[3] L. Y. Gorelik, D. Fedorets, R. I. Shekhter, and M. Jonson, New J. Phys. **7**, 242 (2005).
[4] J. Twamley, D. W. Utami, H. S. Goan, and G. Milburn, New J. Phys. **8**, 63 (2006).
[5] R. H. Blick, H. Qin, H. S. Kim, and R. Marsland, New J. Phys. **9**, 241 (2007).
[6] J. R. Johansson, L. G. Mourokh, A. Yu. Smirnov, and Franco Nori, Phys. Rev. B **77**, 035428 (2008).
[7] H. Park, J. Park, A. K. L. Lim, E. H. Anderson, A. P. Alivisatos, and P. L. McEuen, Nature (London) **407**, 57 (2000).
[8] D. W. Utami, H. S. Goan, and G. J. Milburn, Phys. Rev. B **70**, 075303 (2004).
[9] L. Y. Gorelik, A. Isacsson, M. V. Voinova, B. Kasemo, R. I. Shekhter, and M. Jonson, Phys. Rev. Lett. **80**, 4526 (1998).
[10] D. Fedorets, L. Y. Gorelik, R. I. Shekhter, and M. Jonson, Europhys. Lett. **58**, 99 (2002).
[11] A. Y. Smirnov, L. G. Mourokh, and N. J. M. Horing, Phys. Rev. B **69**, 155310 (2004).
[12] A. Erbe, C. Weiss, W. Zwerger, and R. H. Blick, Phys. Rev. Lett. **87**, 096106 (2001).
[13] C. C. Kaun and T. Seideman, Phys. Rev. Lett. **94**, 226801 (2005).
[14] Y. Azuma, T. Hatanaka, M. Kanehara, T. Teranishi, S. Chorley, J. Prance, C. G. Smith, and Y. Majima, Appl. Phys. Lett. **91**, 053120 (2007).
[15] H. S. Kim, H. Qin, and R. H. Blick, arXiv:0708.1646 (unpublished).
[16] T. Novotný, A. Donarini, and A. P. Jauho, Phys. Rev. Lett. **90**, 256801 (2003).
[17] D. Fedorets, L. Y. Gorelik, R. I. Shekhter, and M. Jonson, Phys. Rev. Lett. **92**, 166801 (2004).
[18] A. Donarini, R. Novotný, and A. P. Jauho, New J. Phys. **7**, 237 (2005).
[19] T. Novotný, A. Donarini, C. Flindt, and A. P. Jauho, Phys. Rev. Lett. **92**, 248302 (2004).
[20] R. Q. Wang, B. G. Wang, and D. Y. Xing, Phys. Rev. Lett. **100**, 117206 (2008).
[21] F. Pistolesi and R. Fazio, Phys. Rev. Lett. **94**, 036806 (2005).
[22] K. H. Ahn, H. C. Park, J. Wiersig, and H. Jongbae, Phys. Rev. Lett. **97**, 216804 (2006).
[23] U. Weiss, *Quantum Dissipative Systems*, Modern Condensed Matter Physics Vol. 10, 2nd ed. (World Scientific, Singapore, 1999).
[24] D. W. Utami, H. S. Goan, C. A. Holmes, and G. J. Milburn, Phys. Rev. B **74**, 014303 (2006).
[25] E. Wigner, Phys. Rev. **40**, 749 (1932).
[26] A. N. Pasupathy, J. Park, C. Chang, A. V. Soldatov, S. Lebedkin, R. C. Bialczak, J. E. Grose, L. A. K. Donev, J. P. Sethna, D. C. Ralph, and P. L. McEuen, Nano Lett. **5**, 203 (2005).